Periodico di Mineralogia (2014), 83, 1, 19-40 DOI: 10.2451/2014PM0002

PERIODICO di MINERALOGIA
established in 1930

An International Journal of
MINERALOGY, CRYSTALLOGRAPHY, GEOCHEMISTRY, ORE DEPOSITS, PETROLOGY, VOLCANOLOGY
and applied topics on *Environment*, *Archaeometry* and *Cultural Heritage*

Geothermobarometry of Al-silicate-bearing migmatites from the Variscan chain of NE Sardinia, Italy: a P-T pseudosection approach

Gabriele Cruciani*, Dario Fancello, Marcello Franceschelli, Massimo Scodina and Maria Elena Spano

Dipartimento di Scienze Chimiche e Geologiche, Università degli Studi di Cagliari, Via Trentino 51, 09127 Cagliari, Italy
*Corresponding author: *gcrucian@unica.it*

Abstract

This paper investigates Al-silicate-bearing migmatite from NE Sardinia by using the P-T pseudosection approach with the aim to determine the P-T conditions of partial melting and those of melt crystallization. P-T pseudosections were calculated in the NCKFMASH system within the P-T range 500-800 °C, 0.1-1.5 GPa by using the average compositions of metapelitic greywacke, average mesosome and average trondhjemitic leucosome, respectively. The P-T pseudosections calculated for the average metapelitic greywacke and for the average mesosome, contoured for melt volume %, Si/Al and Na/K molar ratios in melt point to P-T conditions ~ 700-740 °C, 1.1-1.3 GPa which are indicative of partial melting. The P-T pseudosection calculated for the average composition of trondhjemitic leucosomes, contoured for kyanite and biotite modal content and for X_{Mg} ratio in biotite indicates P-T conditions of 660-730 °C, 0.75-0.90 GPa for the crystallization of the melt. The comparison between the Na/K and Si/Al ratios in leucosomes, and the same ratios modeled for the anatectic melt by an haplogranitic melt model is thus a powerful tool for the reconstruction of P-T conditions of partial melting also in pelitic rocks, provided that leucosomes represent pure melts and are not contaminated by restitic phases or feldspar cumulates.

Key words: Al-silicate-bearing pelitic migmatite; geothermobarometry; P-T pseudosection; anatexis; Variscan Sardinia.

Introduction

P-T path reconstructions for migmatite terrains firstly based on conventional geothermobarometry (Conrad et al., 1988; Sawyer and Barnes, 1988; Palmeri, 1997; Jung et al., 1998; Garcìa-Casco et al., 2001; Acquafredda et al., 2006; Calderón et al., 2007; Cruciani et al., 2008 a,b; Jung et al., 2009) have been recently obtained and discussed on the basis of P-T pseudosection modeling calculated for average, representative rock composition (White et al., 2001; Johnson et al., 2003; Johnson and Brown, 2004) or for the bulk composition of specific samples (Groppo et al., 2009, 2010; Korhonen et al., 2010). In fact, P-T pseudosection approach is the most powerful method currently available to obtain information about the P-T evolution of a wide variety of metamorphic rocks, including migmatites. Recently, Massonne et al. (2013) proposed a P-T pseudosection approach particularly suitable for anatectic rocks, in which the thermodynamic calculations are carried out in two steps: i) study of the mesosome melting, ii) study of the leucosome crystallization. According to this method, P-T pseudosections, calculated for an average composition of mesosome, are used to estimate P-T conditions of the anatectic event, whereas P-T pseudosections calculated for the average bulk composition of leucosomes are used to determine which mineral phases crystallized from the anatectic melt. Massonne et al. (2013) applied this study to amphibole-bearing migmatite from NE Sardinia. At Punta Sirenella, adjacent to the amphibole-bearing migmatite, crop out Al-silicate-bearing pelitic migmatites consisting of sillimanite, kyanite, garnet, plagiolase, quartz, biotite and muscovite. In this paper we extend the geothermobarometric approach of Massonne et al. (2013) to the Al-silicate-bearing pelitic migmatites in order to suggest better constraints on their P-T evolution.

The geothermobarometric results are discussed in the framework of the Sardinia-Corsica Variscan chain.

Geological Setting

The Axial Zone of the Variscan chain of Sardinia (Figure 1a) consists of two metamorphic complexes: the Low to Medium Grade Metamorphic Complex and the High Grade Metamorphic Complex (or Migmatite Complex). The two complexes are separated by the Posada-Asinara tectonic line, interpreted as a major late Variscan sinistral shear line (Elter et al., 1990; Helbing and Tiepolo, 2005; Giacomini et al., 2005; Padovano et al., 2012).

The Low to Medium Grade Metamorphic Complex is mostly made up of metapelite, metagreywacke, micaceous quarzites, metavolcanics and metabasite metamorphosed under greenschist and amphibolite facies conditions (Franceschelli et al., 1989; Costamagna et al., 2012). Chloritoid schist from this Complex underwent a HP-metamorphic imprint before the Barrovian amphibolite-facies metamorphism (Cruciani et al., 2013).

The Migmatite Complex consists of a suite of multideformed migmatites, micaschists, paragneisses, orthogneisses, metabasites with eclogite and granulite facies relics (Franceschelli

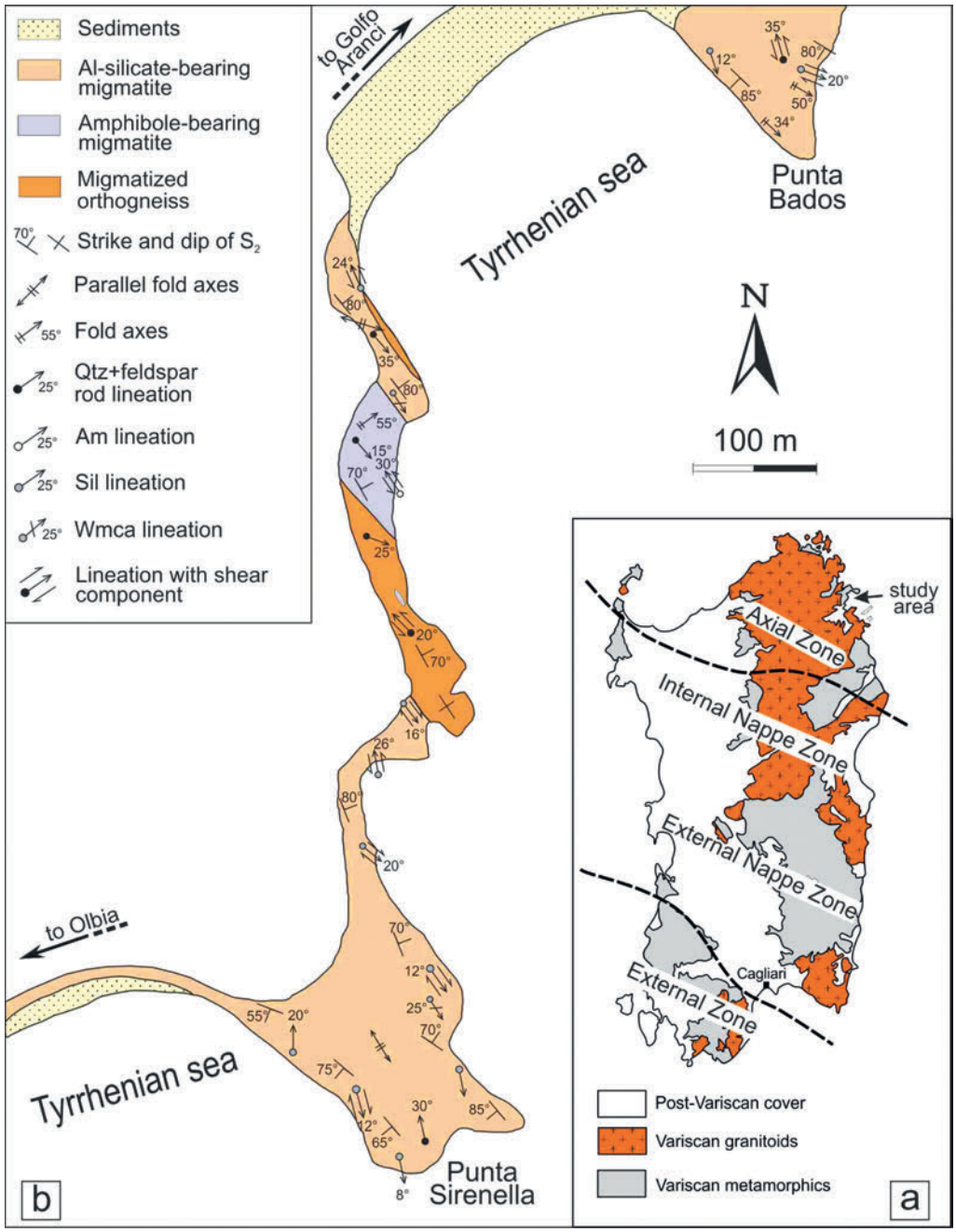

Figure 1. a) tectonic sketch map of the Variscan basement of Sardinia (adapted from Carmignani et al., 2001); b) geological sketch map of Punta Sirenella-Punta Bados area (adapted from Cruciani et al., 2008a).

et al., 1989, 1998; Elter et al., 1986; Cruciani et al., 2001; Ricci et al., 2004), and calc-silicate rocks. An extended review of Variscan orogeny in Sardinia can be found in Franceschelli et al. (2005).

The migmatites have the composition of immature, quartz-rich clastic sediments, mainly wackes to arkoses with subordinate pelites originating from the weathering and erosion of felsic Ordovician magmatic rocks (Giacomini et al., 2006).

U-Pb zircon ages of the metasediments scatter between 0.32 and 3.0 Ga (Giacomini et al., 2006). Two main clusters in this age spectrum were observed at 450-480 Ma and 550-650 Ma. Variscan ages are rare and only related to thin rims around older zircon cores (Giacomini et al., 2006).

Partial melting in pelitic migmatite started in the kyanite field at about 700-720 °C and 0.8-0.9 GPa, and was followed by re-equilibration at 650-670 °C and 0.4-0.6 GPa, with incipient growth of fibrolite needles, in turn followed by the formation of late cross-cutting muscovite. The trondhjemitic leucosomes were generated by H_2O-fluxed melting at 700 °C of a greywacke to pelitic-greywacke metasedimentary source (Cruciani et al., 2008a).

Field occurrence and petrographic features

Field occurrence, petrographical features, and bulk chemistry of the Al-silicate-bearing migmatites from Punta Sirenella are discussed in detail by Cruciani et al. (2008a). In this section a brief summary of the main results of this paper will be provided.

The Al-silicate-bearing migmatites cropping out between Punta Sirenella and Punta Bados (Figure 1b), NE of Olbia are mostly layered rocks containing 3-5 vol.% of centimeter-thick stromatic leucosomes (Figure 2 a,b) which are mainly trondhjemitic and rarely granitic in composition. The Al-silicate-bearing migmatite contains folded calc-silicate nodules and metasedimentary layers that escaped partial melting (Figures 2 c,d). The migmatites are affected by at least three main deformations (D_1, D_2, D_3) (Figures 2 b,c,d). D_1, not clearly recognizable in the field, is documented by the transposition of centimeter-sized leucosomes. The D_2 phase is revealed by N140° striking isoclinal folds with a SE dip of 2-18° (Figure 2b). On the XY plane of the S_2 schistosity, three different mineralogical lineations can be recognized: the first one consists of rods and/or pencils of plagioclase+quartz; the second one is a fibrolite+quartz mineralogical lineation (Figure 3a); the third one consists of muscovite (Figure 3b), sometimes overprinting the previous lineation (Cruciani et al., 2008a). The D_2 phase is followed by a late deformation (D_3) characterized by open folds and pervasive crenulation cleavage.

The leucosomes, with length varying from a few centimeters up to 1-2 m, are often deformed, stretched and/or strongly folded. Discontinuous to boudin-shaped leucosomes, parallel to the main schistosity also occur. Leucosomes consist of quartz (40-50%), plagioclase (35-45%), biotite ($\leq$ 5%), $\pm$ garnet (< 1%), $\pm$ kyanite (< 5%), $\pm$ fibrolite (< 10%), K-feldspar ($\leq$ 1%), and retrograde muscovite (5-10%) (Figures 3 c,d). Accessory minerals are zircon, apatite, rutile and monazite.

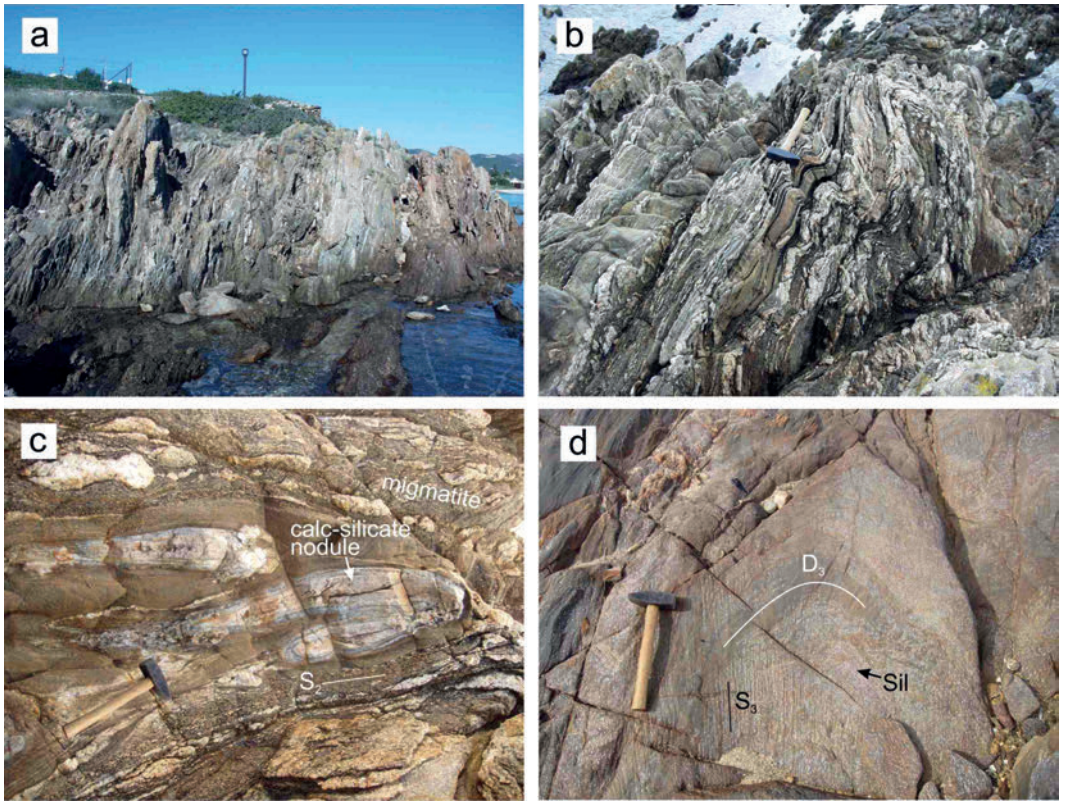

Figure 2. a), b) appearance of the Al-silicate-bearing migmatites at the outcrop scale. The migmatite shows a layered and deformed structure; c) calc-silicate nodule hosted by the Al-silicate-bearing migmatites. Elongation of the nodule is parallel to the S_2 schistosity; d) metapelitic greywacke showing alternation between sillimanite-rich and sillimanite-poor layers. Fibrolite needles are oriented parallel to S_3 foliation.

The rare granitic leucosomes differ from trondhjemitic ones only in the increase in modal content of K-feldspar, up to 25%.

The mesosome (proximal host of Cruciani et al., 2008a) consists of plagioclase (25-35%), quartz (30-40%), biotite (15-20%), ± kyanite (up to 4-5%), ± garnet (up to 2-3%), ± fibrolite (up to 20%), coarse-grained muscovite (10-20%) and zircon, apatite, rutile and monazite as accessory phases. Sometimes mesosomes only consist of quartz, plagioclase, biotite and muscovite. The melanosomes are characterized by a high amount of biotite.

Plagioclase crystals show a oligoclasic core (~ An_{20-23}) surrounded by a discontinuous albite rim of variable thickness. Matrix biotite, biotite trails partially replaced by fibrolitic sillimanite, and retrograde biotite growing on garnet have Si content ~ 5.3-5.4 a.p.f.u.. Ti ranges from 0.3 to 0.4 a.p.f.u. in matrix biotite, whereas in biotite

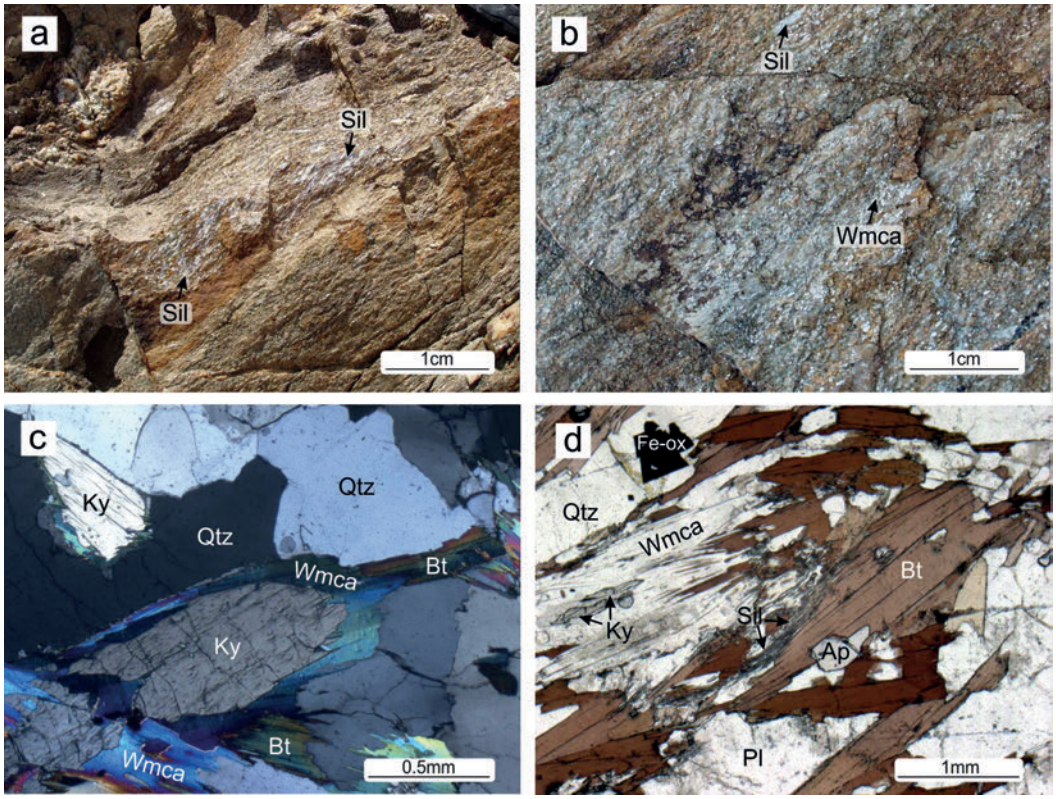

Figure 3. a) sillimanite lineation along the XY plane of S_2 schistosity; b) late crosscutting muscovite along the XY plane of S_2 schistosity; c) kyanite surrounded by retrograde muscovite in a matrix mainly made up of quartz, plagioclase, and biotite. Photomicrograph, leucosome sample B61, crossed polars; d) biotite trail defining the S_2 schistosity. Biotite growing with fibrolitic sillimanite is surrounded by a quartz-feldspathic matrix made up of plagioclase and quartz. Photomicrograph, leucosome sample B31, single polar.

replacing garnet, it is 0.15 a.p.f.u. X_{Mg} ranges between 0.42 and 0.52 in biotite from the matrix, and is close to 0.50 in biotite replacing garnet.

Garnet composition is Alm_{65-72}, Pyr_{12-17}, Grs_{3-5}, $Sps_{8-20\ mol.\%}$. Mn shows asymmetric zoning, with a general increase in spessartine content from core to rim up to 6-7% accompanied by a counterbalancing decrease in Fe and Mg, and a fairly constant Ca content.

Muscovite growing around kyanite has low Ti (0.005-0.029 a.p.f.u.) content, as well as low Fe (0.06 a.p.f.u.) and Mg content (0.08 a.p.f.u.). Crosscutting muscovite from the matrix have Si content between 6.04 and 6.15 a.p.f.u., Ti content from 0.03 to 0.18 a.p.f.u. and Mg between 0.08 and 0.16 a.p.f.u. Fe shows a narrow range of variation, between 0.09 and 0.14 a.p.f.u.

Methods

P-T pseudosection calculations were carried out with PERPLE_X 6.6.7 following the approach of Connolly (1990) and the internally consistent thermodynamic dataset and equation of state for H_2O of Holland and Powell (1998, revised 2004). P-T pseudosections were calculated in the NCKFMASH system within the P-T range 500-800 °C, 0.1-1.5 GPa. Iron was assumed to be Fe^{2+} because Fe^{3+} content in the main minerals (garnet, biotite, white mica) is negligible and Fe^{3+}-bearing oxides occurr in trace amounts. CaO was reduced according to P_2O_5 content in the rocks, on the likelihood that phosphorus binds exclusively to calcium in ideally-composed apatite.

The phases considered in the calculation were biotite (Bt), potassic white mica (Wmca), Na-rich white mica (Pa), chlorite (Chl), garnet (Grt), staurolite (St), cordierite (Crd), orthopyroxene (Opx), plagioclase (Pl), albite (Ab), K-feldspar (Kfs), kyanite (Ky), sillimanite (Sil), andalusite (And), zoisite (Zo), quartz (Qtz), and melt (L). Solid solution models are those of Holland and Powell (1998) for white mica, garnet, staurolite, Powell and Holland (1999) for biotite, Holland et al. (1998) for chlorite, Thompson and Hovis (1979) for alkali feldspar and Newton et al. (1981) for plagioclase. The haplogranitic melt model by Holland and Powell (2001) and White et al. (2001) was used. Calculations were performed using the H_2O content derived from the LOI value

Table 1. Bulk compositions of average metapelitic greywacke, average mesosome and average leucosome used in P-T pseudosection calculations. XRF whole rock data in wt.% are recalculated into mole % after apatite correction. Average mesosome and average leucosome compositions have been obtained from mesosome and leucosome samples from Cruciani et al. (2008a).

	Average metapelitic greywacke		Average mesosome		Average leucosome	
	wt.%	mol.%	wt.%	mol.%	wt.%	mol.%
SiO_2	61.46	64.55	63.08	66.06	72.20	76.05
TiO_2	0.90	-	0.92	-	0.28	-
Al_2O_3	18.25	11.39	16.76	10.35	15.38	9.55
FeO_{tot}	6.30	5.70	6.05	5.30	1.97	1.74
MnO	0.06	-	0.09	-	0.03	-
MgO	3.33	5.06	3.11	4.86	0.89	1.40
CaO	0.73	0.65	1.45	1.35	2.30	2.46
Na_2O	2.78	2.53	2.60	2.64	4.43	4.52
K_2O	3.39	2.53	2.93	1.96	1.23	0.83
P_2O_5	0.12	-	0.19	-	0.09	-
LOI	2.13	7.59	2.14	7.48	0.98	3.45

and the fluid phase was considered as pure H_2O. Different H_2O contents have also been considered with the aim to obtain information on the phase relations at various H_2O contents. Bulk rock compositions used in P-T pseudosection calculations are shown in Table 1.

Results of P-T pseudosection calculation

Modeling the migmatite protolith

In the migmatite sequence of Punta Bados some levels (up to a few tens of meters in thickness) are characterized by a regular alternation of fibrolite-rich levels (with millimetric fibrolite nodules visible to the naked eye) and fibrolite-free levels (Figure 2d). The pervasive foliation S_2, oriented parallel to the fibrolite nodules, is partially overprinted by an S_3 crenulation cleavage at high angle. These metasedimentary levels, which lack any evidence of partial melting, appear to have escaped from anatexis so that they can be considered the best approximation to the migmatite protolith.

From these levels we selected five samples of metapelitic greywacke (classification according to the SiO_2/Al_2O_3 vs. K_2O/Na_2O diagram after Wimmenauer, 1984) of which the average bulk rock composition analyzed by XRF is reported in Table 1. The P-T pseudosection calculated for the average bulk composition of metapelitic greywacke is shown in Figure 4. The pseudosection is dominated by quadri- and tri-variant fields (intermediate and light blue fields) with some minor divariant (white) and pentavariant (dark blue) fields mostly restricted at intermediate P-T and at LP-HT conditions, respectively. Biotite is present in almost the entire investigated P-T range, except for a small range between 750-800 °C, 0.1-0.4 GPa where cordierite and orthopyroxene are the main stable mafic phases. The minimum temperature for melt is 650 °C at ~ 0.4 GPa; at all different pressures melt appears at slightly higher temperature values. Figure 4b shows contour lines representing melt abundance (vol.%) in melt-bearing multivariant fields, whereas Figures 4 c,d report contour lines representing melt composition in terms of Si/Al and Na/K molar ratios, respectively. The P-T pseudosection predicts that, at the P-T conditions of anatexis close to 1.0-1.3 GPa and 700 °C, the anatectic melt should be characterized by Si/Al and Na/K molar ratios ~ 3.8 and ~ 8-9, respectively. The Si/Al and Na/K molar ratios in the Punta Sirenella trondhjemitic leucosomes range as follows: Si/Al = 3.6-4.8, average 4.0; Na/K = 3.1-8.8, average 6.1. (Cruciani et al., 2008a). Thus, the Si/Al ratio in the leucosomes matches well the predicted values, whereas the Na/K ratio appears to be, on average, a little lower than expected. It is also worthy of note that Cruciani et al. (2008a) estimated a volume proportion of 3-5 vol.% of leucosomes into the migmatite, whereas the expected melt percentage would be ~ 5-7 vol.% at the estimated P-T conditions of anatexis. However, a significant effect on the P-T position of contour lines showing the volume percentage of the melt has been observed with different H_2O content, resulting in an increase of melt vol.% with rising water content.

Modeling the mesosome

A P-T pseudosection (Figure 5a) was calculated for the average composition of mesosomes (proximal hosts in Cruciani et al., 2008a) of the Al-silicate-bearing migmatites (Table 1). Figures 5 b,c,d show contour lines representing melt content in vol.%, and melt composition in terms of molar ratios of Si/Al and Na/K in the melt, respectively. The pseudosection of Figure 5a is similar to that shown in Figure 4a, suggesting that, on average, the composition of mesosome resembles that of unmelted metapelitic-greywacke of Punta Bados. However, the following main differences can be envisaged between the two P-T pseudosections:

(i) the solidus curve appears at lower temperatures (20-30 °C) in the P-T pseudosection calculated for the average bulk composition of metapelitic greywacke compared to the solidus curve in the P-T pseudosection calculated for the average composition of the mesosomes (i.e. average metapelitic greywacke is more fertile than average mesosome).

(ii) at high pressure (> 0.9 GPa), the melt proportion (vol.%) produced by anatexis of the average metapelitic greywacke is slightly lower than that can be obtained from the partial melting of the average mesosome composition.

In order to define the P-T conditions of anatexis, contour lines of Si/Al and Na/K ratios in melt are compared with the same ratios observed in leucosomes. The Si/Al ratio in trondhjemitic leucosomes ranges from 3.6-4.8 with an average of 4.01, whereas the Na/K ratio varies in the 3.1-8.8 range, with average 6.13. The average values of the trondhjemitic leucosomes define P-T conditions of about 680 °C and 1.1 GPa. The wide range of variation of the Si/Al and Na/K ratio of the trondhjemitic leucosomes could be related to the fact that these leucosomes do not represent pure melts (Cruciani et al., 2008a). More precise P-T constraints can be obtained from the Si/Al and Na/K ratios averaged from two leucosomes (270LT, 32LT) that do not show significant entrainment of restitic phases (Cruciani et al., 2008a). The average values of the molar ratios in the 270LT, 32LT trondhjemitic leucosomes (Si/Al = 3.88; Na/K = 4.07) intersect at the transition between the Wmca+Pl+Grt+Bt+Qtz+L field and the Wmca+Pl+Grt+Bt+Qtz+Ky+L field of the P-T pseudosection at P ~ 1.1-1.3 GPa and T ~ 700-740 °C (Figure 5), where a 9-11 vol.% melt is expected (Figure 5b).

Modeling the trondhjemitic leucosomes

In migmatite terrains it is very common that most leucosomes are not pure melts but feldspar cumulates. In addition, during the segregation of anatectic melt, some minerals, possibly of peritectic origin, and/or some of the wall rock material can become entrained in the melt (Taylor and Stevens, 2010). In such cases, using the bulk composition of a leucosome as a proxy to melt composition for P-T pseudosection modeling is unlikely to have much meaning.

Hence, the selection of leucosomes to be used as proxy of pure melt composition in P-T pseudosection modeling is a crucial point that deserves special attention. Among the trondhjemitic leucosomes published by Cruciani et al. (2008a), four leucosomes show evidence of entrainment of restitic phases, whereas the other

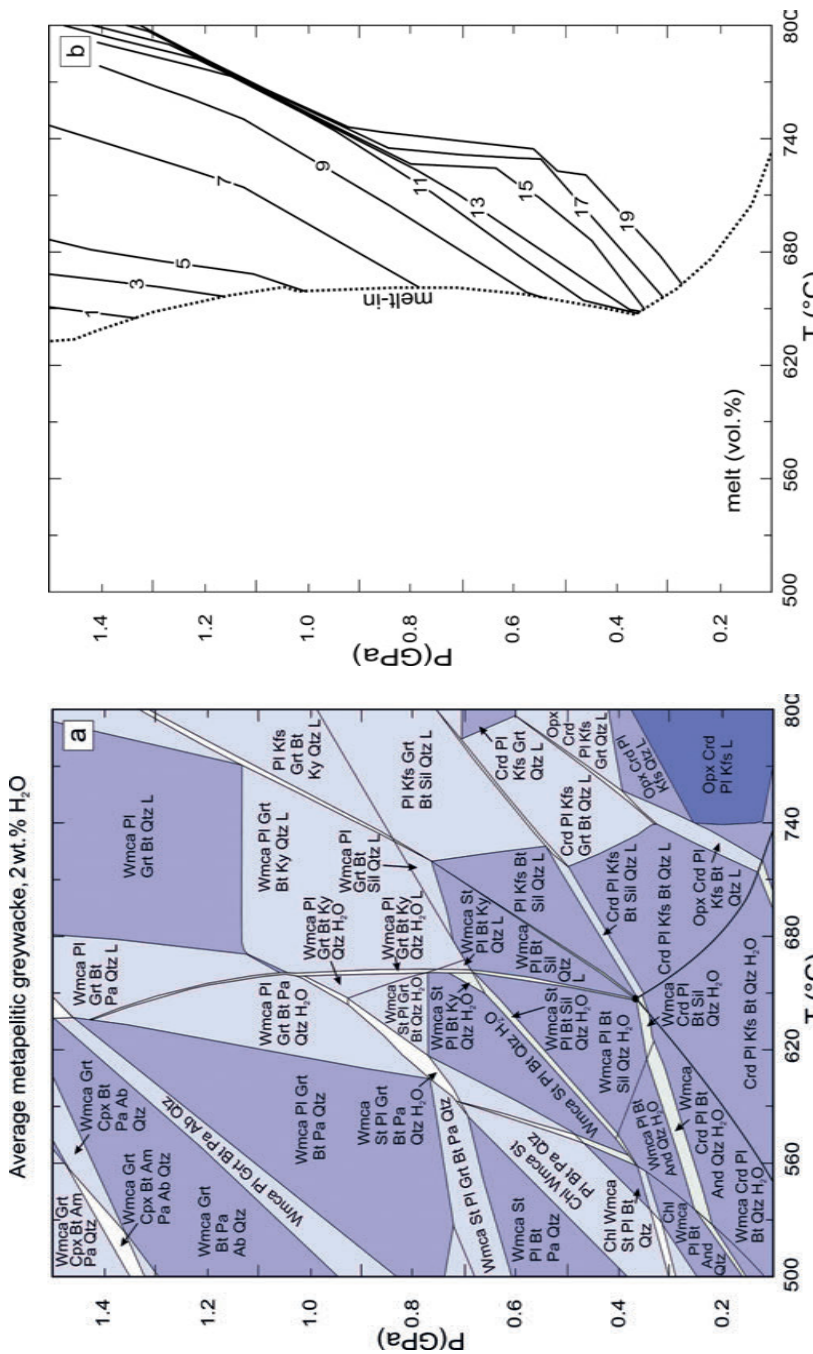

Figure 4. a) P-T pseudosection calculated in the NCKFMASH system for the composition of average metapelitic greywacke with ~ 2 wt.% H_2O; b) contour lines showing melt content in vol.%; c) contour lines showing Si/Al molar ratio in the melt, and d) contour lines showing Na/K molar ratio in the melt. Mineral abbreviations according to Fettes and Desmons (2007).

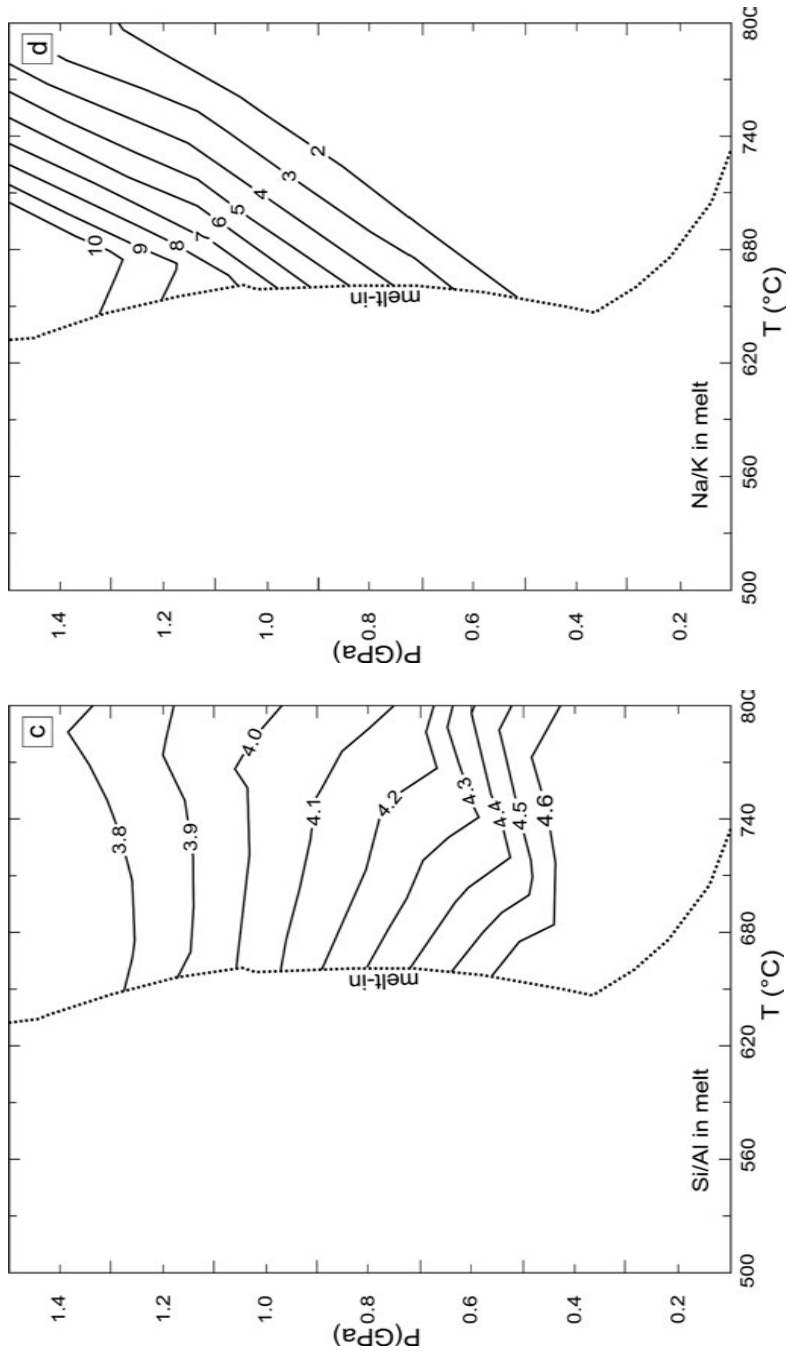

Figure 4. Continued...

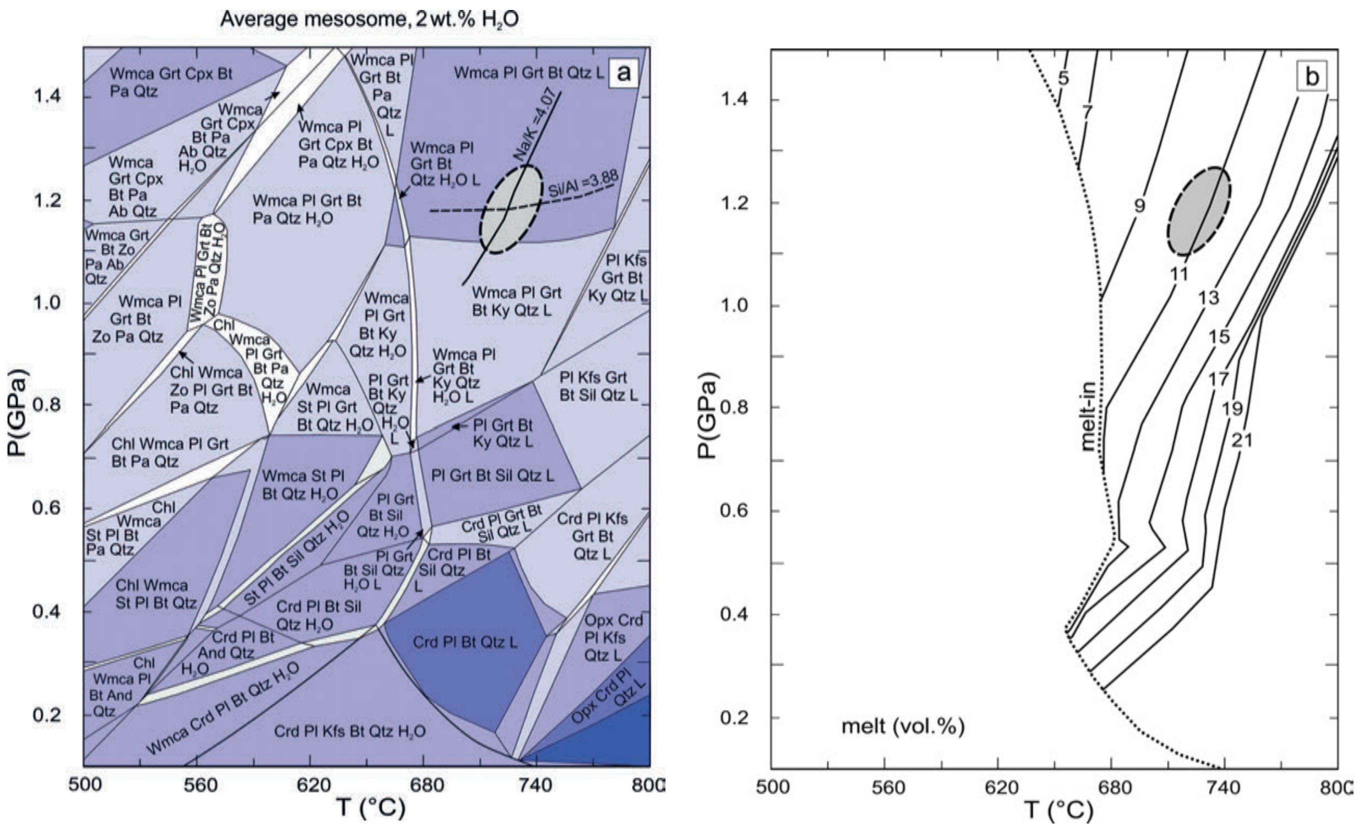

Figure 5. a) P-T pseudosection calculated in the NCKFMASH system for the average composition of trondhjemitic leucosomes with ~ 1.5 wt.% H_2O (composition from Cruciani et al., 2008a); (b) isomodes showing kyanite and sillimanite modal amount in vol.%; c) isomodes showing biotite modal amount in vol.%; d) contour lines showing X_{Mg} ratio in biotite. Grey ellipse represents P-T conditions of melt crystallization.

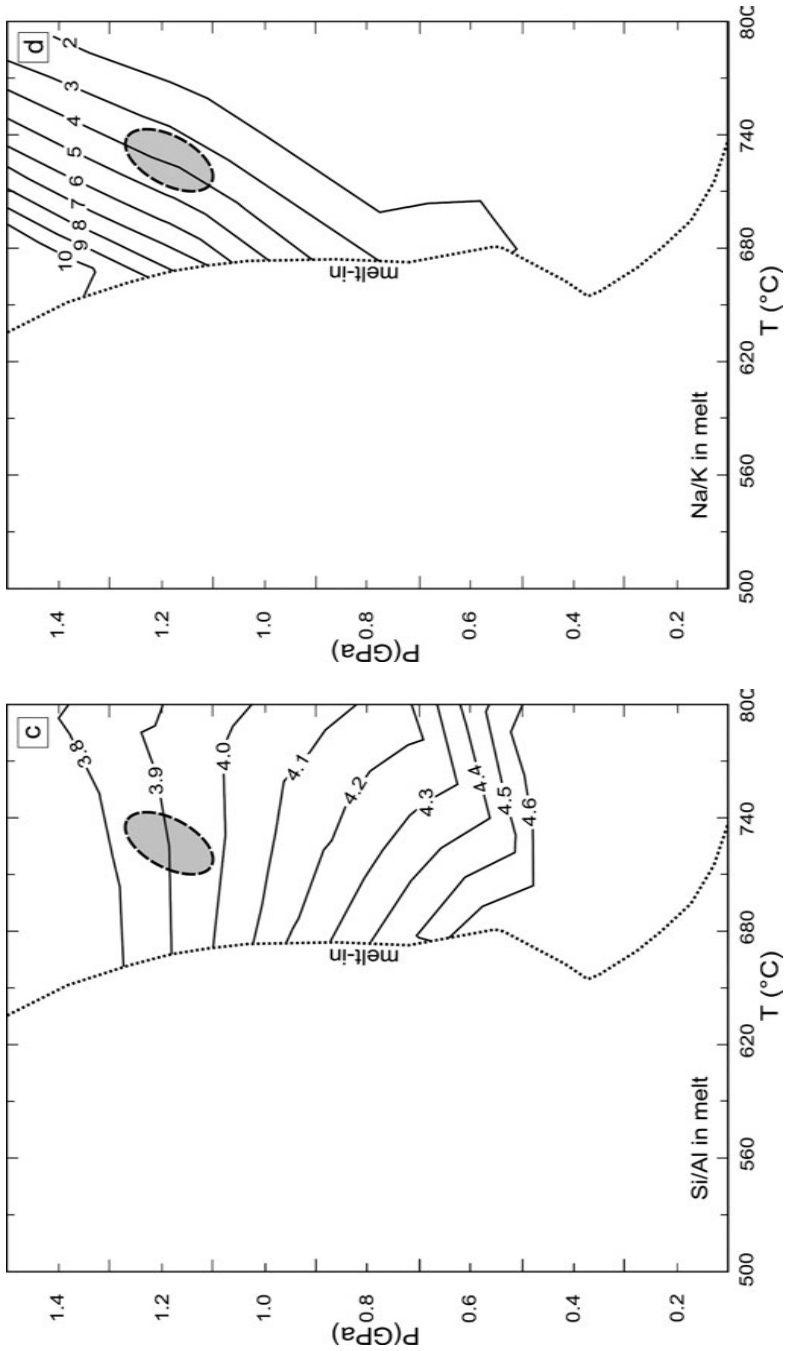

Figure 5. Continued...

two samples are characterized by geochemical evidences of zircon entrainment.

In order to reduce the influence of the restitic phases, the P-T pseudosection shown in Figure 6a is calculated for a bulk composition averaged from the trondhjemitic leucosomes reported by Cruciani et al. (2008a) (Table 1). Figures 6 b,c,d show the modal content of kyanite, sillimanite, biotite (vol.%) and biotite X_{Mg} ratio, respectively. The comparison of isomodes (Figures 6 b,c) representing the modal content of kyanite, sillimanite and biotite with the modal abundance actually observed in trondhjemitic leucosomes (kyanite between 3-4 vol.%, biotite < 5vol.%) and comparison of compositional isopleths of X_{Mg} in biotite (Figure 6d) with X_{Mg} ratio in leucosome biotite (X_{Mg} = 0.42-0.52, Cruciani et al., 2008a) provide indication of P-T conditions of crystallization of the melt at ~ 660-730 °C, ~ 0.75-0.90 GPa (error ellipses in Figure 6). Compositional isopleths representing almandine and grossularite components in garnet (not shown) reveal that the derived P-T conditions are also in agreement with the almandine and grossularite content (Alm: 65-70 mol%; Grs: 4-5 mol%) reported for garnet in trondhjemitic leucosomes by Cruciani et al. (2008a).

Discussion

The P-T conditions and P-T path estimated for the Al-silicate-bearing migmatite of Punta Sirenella-Punta Bados with the pseudosection approach is shown in Figure 7 together with the P-T path of the same Al-silicate-bearing migmatite based on conventional geothermobarometry redrawn from Cruciani et al. (2008a). The two P-T paths are compared with the P-T path proposed by Massonne et al. (2013) for the adjacent amphibole-bearing migmatite, with which the migmatite shared a common metamorphic history. According to the method proposed by Massonne et al. (2013), we report P-T estimates represented by two ellipses in Figure 7. The first ellipse defines the P-T conditions of partial melting whereas the second one represents the P-T conditions of the melt crystallization, i.e. when the melt crossed the solidus curve towards low temperatures. This reconstruction appears to be compatible with the P-T path reported by Cruciani et al. (2008a). However, two main differences can be observed: 1) the P- T estimates for the partial melting obtained with the P-T pseudosection approach are higher than those obtained by Cruciani et al. (2008a) with conventional geothermobarometry; 2) the P-T path from Cruciani et al. (2008a) is constrained also at low temperatures. The discrepancy between the two P-T estimates for partial melting is only apparent. In fact, the P-T path of Al-silicate-bearing migmatite was reconstructed by Cruciani et al. (2008a) on the basis of the P-T estimates obtained by using the Grt-Bt geothermometer and the GASP (garnet-Al_2SiO_5-plagioclase-quartz) geobarometer applied to the composition of garnet core and rim. These authors suggested that the highest temperatures obtained by conventional geothermobarometry may be considered close to, but not at the thermal peak of Variscan metamorphism in Sardinia. Similarly, they suggest that pressure estimates by the GASP

geobarometer probably do not reflect peak pressure during partial melting. Thus, the P-T path reconstruction of Cruciani et al. (2008a) probably reflects P-T conditions along the cooling trajectory of the rocks from partial melting (represented by the garnet core) to the last re-equilibration under amphibolite facies. The last part of the P-T path was constrained by the authors on the basis of fluid inclusion data.

The P-T estimates for the partial melting (T ~ 700-740 °C, P ~ 1.1-1.3 GPa) and for the melt crystallization (~ 660-730 °C, ~ 0.75-0.90 GPa) obtained for the Al-silicate-bearing migmatite with the P-T pseudosections presented here are also comparable with those proposed by Massonne et al. (2013) for the nearby amphibole-bearing migmatites (partial melting: 700 °C, 1.3 GPa; complete crystallization of the melt: 680 °C, 0.9 GPa) with which the sedimentary-derived migmatites under study has shared most of their metamorphic and deformative history. According to Cruciani et al. (2008a) only the retrograde part of the migmatite P-T path can be reconstructed, because peak metamorphic conditions obliterated the prograde part. The prograde part of the P-T path was tentatively reconstructed by Giacomini et al. (2005; their Figure 12b) for the migmatitic paragneiss and felsic orthogneiss (Gneiss Complex) cropping out in the Golfo Aranci area, NE Sardinia.

P-T pseudosection calculation indicates that the protolith of Al-silicate-bearing migmatite underwent partial melting at high-pressure conditions with approximately 1.5-2.0 wt.% of H_2O. Although the melt content is strongly dependent on the H_2O content of the rock before partial melting, the estimated water content appears to be compatible with the observed leucosome vol.% at the outcrop scale, which were estimated to be ~ 3-5 vol.% by Cruciani et al. (2008a). Subsequently, pressure release and slight cooling resulted in the crystallization of the leucosome melt to form, among other phases, kyanite and biotite. The further retrograde P-T evolution cannot be assessed from the P-T pseudosection analyses of the studied rocks. However, some thermobarometric constraints can be obtained from the comparison of the expected, and actually observed, modal abundances of retrograde mineral phases (i.e. sillimanite and muscovite). In particular it is interesting to determine whether fibrolite formed in coexistence of the melt phase or if it formed when the melt was already crystallized. The observed modal abundance of fibrolite in the trondhjemitic leucosomes is < 10 vol.% whereas in mesosomes it reaches up to 20 vol.%. Since the sillimanite in coexistence with the melt predicted by isomodes in Figure 6b reaches up to a maximum of 2% modal abundance, the high abundance of this mineral in the migmatites cannot be explained solely by partial melting: according to what was already observed by Cruciani et al. (2008a), the fibrolitic sillimanite which forms folia, patches and veinlets on the S_2 schistosity (Figure 3a) might have formed with the contribution of a large-scale metasomatic process, such as base cation leaching due to acid volatiles.

As regards the muscovite formation, the isomodes (not shown in Figure 6) reveal that,

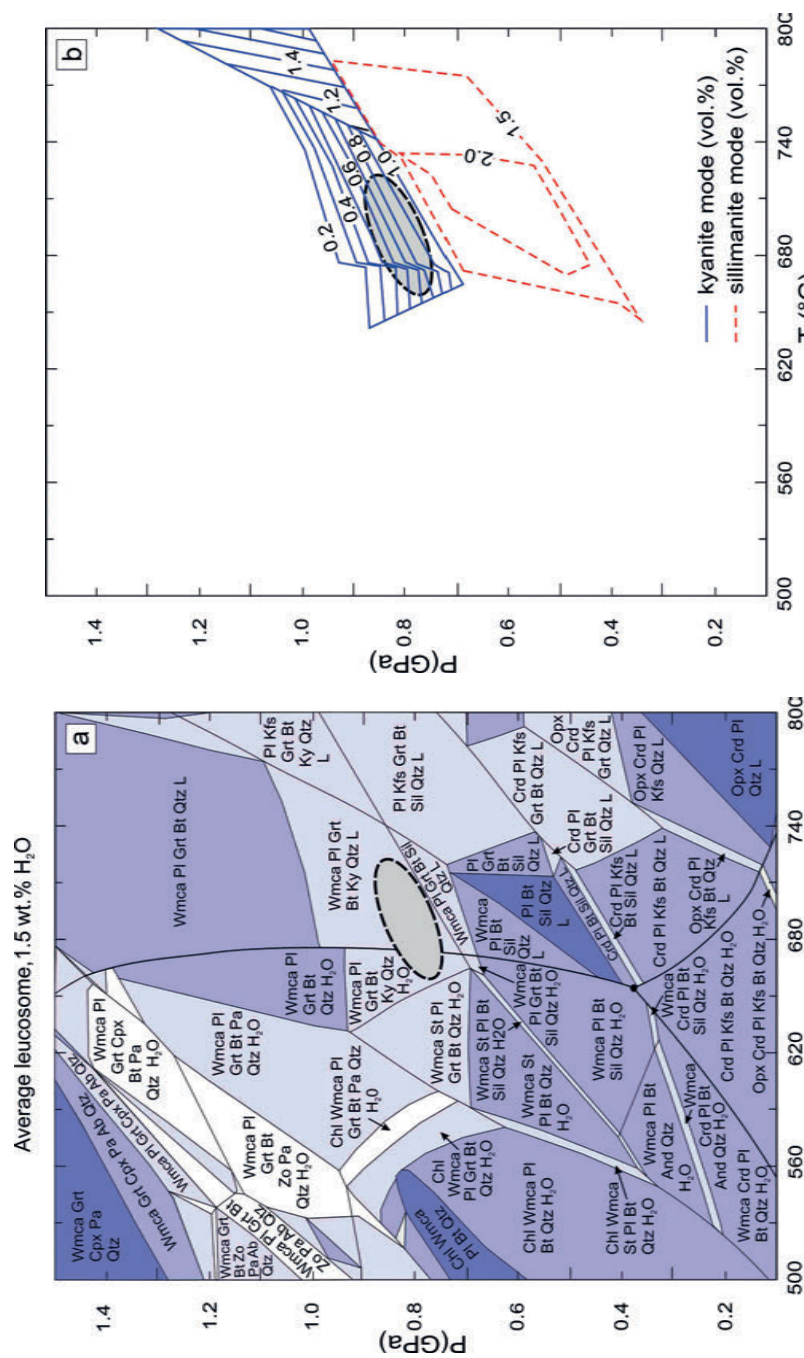

Figure 6. a) P-T pseudosection calculated in the NCKFMASH system for the average composition of trondhjemitic leucosomes with ~ 1.5 wt.% H_2O (composition from Cruciani et al., 2008a); (b) isomodes showing kyanite and sillimanite modal amount in vol.%; c) isomodes showing biotite modal amount in vol.%; d) contour lines showing X_{Mg} ratio in biotite. Grey ellipse represents P-T conditions of melt crystallization.

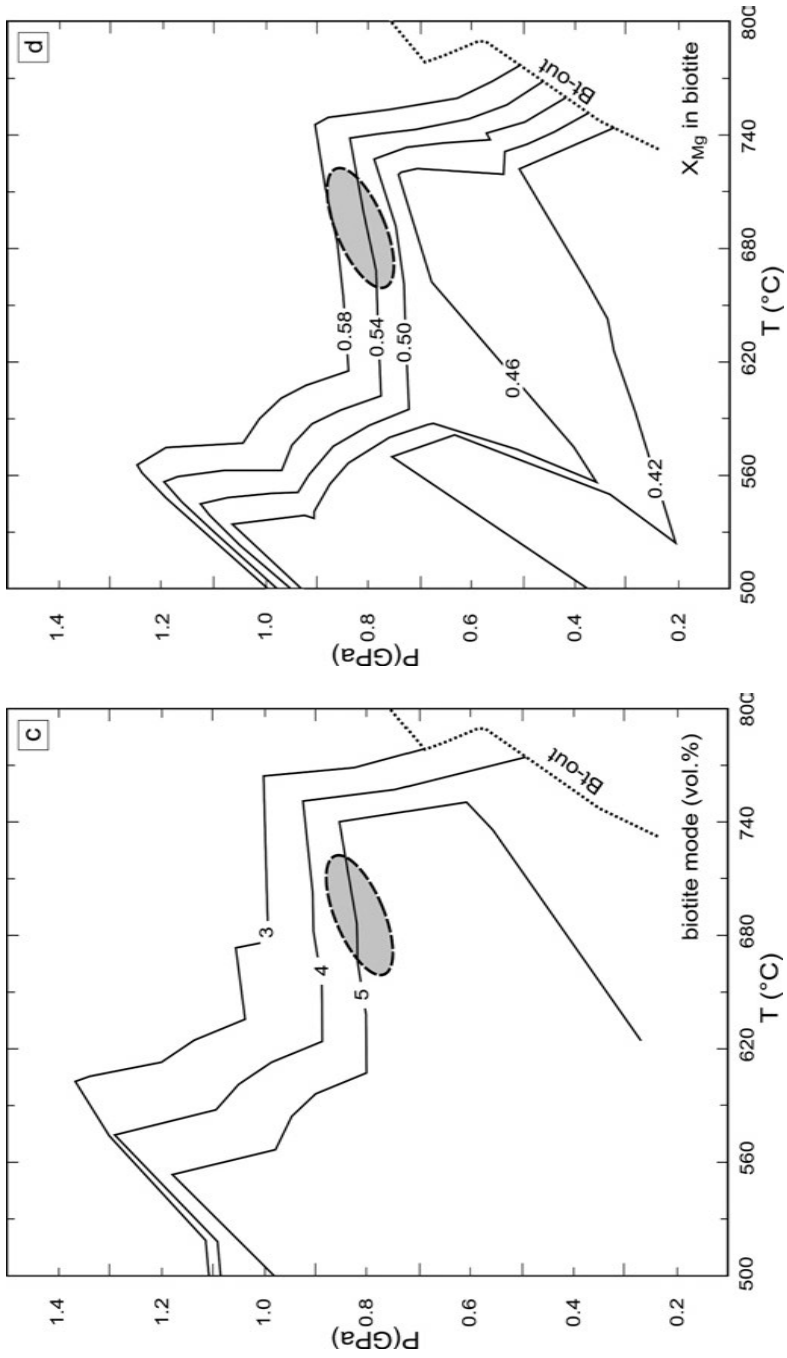

Figure 6. Continued...

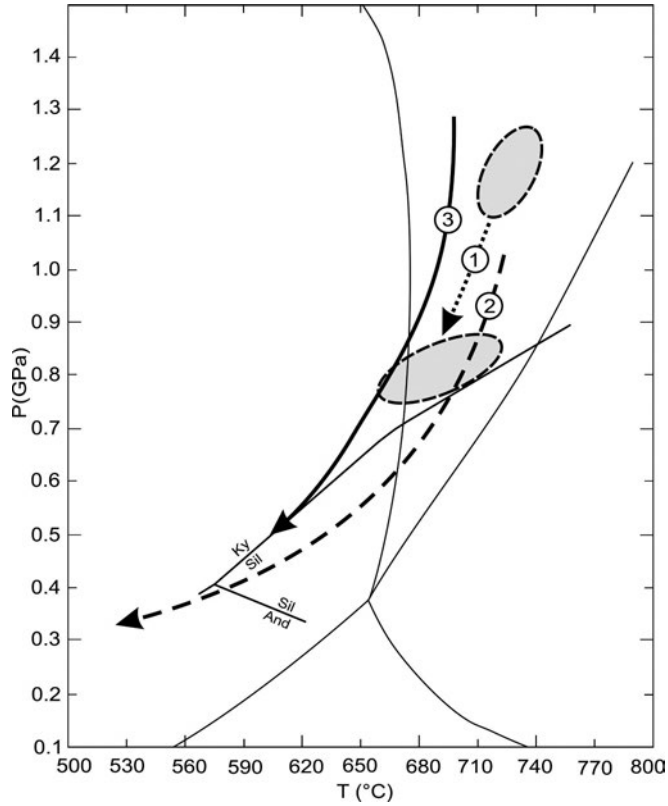

Figure 7. P-T path of the Al-silicate-bearing migmatites of Punta Sirenella-Punta Bados reconstructed with the P-T pseudosection approach (P-T path 1) compared to the P-T path obtained for the same rocks by conventional geothermobarometry (P-T path 2; Cruciani et al., 2008a) and to that of the neighbouring amphibole-bearing migmatite (P-T path 3; Massonne et al., 2013). Melting curves and aluminium silicate triple point are redrawn from Figure 6a.

along the P-T path of the Al-silicate-bearing migmatite, potassic white mica decreases in modal abundance until it coexists with the melt phase. Subsequently, when the melt disappears, the modal content of white mica starts to increase. This observation indicates that retrograde muscovite starts to form when the P-T path of the rocks passes above the invariant point IP1 of the NaKFMASH system, out from the stability field of the melt phase. In fact, Si content in muscovite is only compatible with multivariant P-T fields at subsolidus P-T conditions (i.e. on the left hand side of the H_2O fluxed melting reaction), documenting that this mineral grew in response to retrograde back reactions.

Along with the migmatites described in this paper, in the metamorphic basement between Olbia and Golfo Aranci the Variscan rocks consist of a suite of migmatite and metabasite

with granulite and eclogite facies relics. These rocks record different peak temperature and peak pressure conditions. The amphibole-bearing migmatites record P-T conditions of partial melting very close to 1.3 GPa and 700 °C (Massonne et al., 2013). Giacomini et al. (2005) estimated that migmatite formation occurred under granulite facies metamorphism at 680-750 °C and 0.8 GPa.

The eclogites embedded in the migmatites underwent peak pressure under eclogite facies P-T conditions of 650 °C and 1.9 GPa (Giacomini et al., 2005) which are in part similar to those estimated by Cruciani et al. (2011) for the eclogitic rocks of Punta Orvili NE Sardinia (620 < T < 650 °C, 1.9 < P < 2.1 GPa) and by Cruciani et al. (2012) for the Punta de li Tulchi eclogites (660-700 °C, 1.7-2.1 GPa). Ultramafic amphibolites in the migmatite preserve granulite facies relics at T = 700-740 °C, P ~ 0.8-1.0 GPa (Ghezzo et al., 1979; Franceschelli et al., 2002).

In southeastern Corsica, Giacomini et al. (2008) describe the lower crust sequences of the Variscan high-grade basement between Solenzara and Porto Vecchio tectonically juxtaposed along middle crustal rocks during the extrusion of the orogenic roots of the chain. According to these authors, these rocks have undergone different P-T conditions (eclogite?, HP-granulite, and amphibolite facies) at different times reflecting the progressive migration of the orogenic front. Several analogies can be envisaged between NE Sardinia and SE Corsica. In both areas, migmatite, eclogitic and granulitic rocks have undergone different P-T conditions. According to Giacomini et al. (2008), the data from SE Corsica are consistent with an exhumation driven by tectonic channel flow at the bottom of the upper plate. In this scenario a system of intracontinental orogen-parallel shear zones developed under a transpressive dextral tectonic regime causing the exhumation on the entire sequence. Similarly, in NE Sardinia, the juxtaposition of rocks with different P-T conditions can be related to exhumation of HT rocks along dextral transpressive shear zones, such as those recently described by Elter et al. (2010).

Concluding remarks

The P-T pseudosection analysis of the Al-silicate-bearing migmatites from Sardinia allows to determine the P-T conditions of partial melting as well as those of melt crystallization. P-T conditions of partial melting have been estimated at 1.1-1.3 GPa, 700-740 °C whereas those of the crystallization of the leucosome melt are 660-730 °C, 0.75-0.90 GPa. The P-T conditions representative of the partial melting event do not significantly differ from those estimated by Cruciani et al. (2008a) by means of conventional geothermobarometry (700-720 °C and 0.8-0.9 GPa). The geothermobarometric approach based on the modeling of Si/Al and Na/K molar ratios in the melt is thus applicable also to pelitic rocks that underwent partial melting and subsequent retrograde re-equilibration in amphibolite facies.

Acknowledgements

We would like to thank the Regione Autonoma della Sardegna, Progetti di Ricerca L.R. 7/2007-

annualità 2010 for their financial support to M. Franceschelli. Two anonymous reviewers are kindly acknowledged for suggestions and helpful comments.

References

Acquafredda P., Fornelli A., Paglionico A. and Piccarreta G. (2006) - Petrological evidence for crustal thickening and extension in the Serre granulite terrane (Calabria, southern Italy). *Geological Magazine*, 143, 145-163.

Calderón M., Hervé F., Massonne H.-J., Tassinari C.G., Pankhurst R.J., Godoy E. and Theye T. (2007) - Petrogenesis of the Puerto Edén Igneous and Metamorphic Complex, Magallanes, Chile: Late Jurassic syn-deformational anatexis of metapelites and granitoid magma genesis. *Lithos,* 93, 17-38.

Carmignani L., Oggiano G., Barca S., Conti P., Salvadori I., Eltrudis A., Funedda A. and Pasci S. (2001) - Geologia della Sardegna. Note illustrative della Carta Geologica della Sardegna a scala 1:200000: Memorie descrittive della Carta Geologica d'Italia, 60, 283 pp.

Connolly J.A.D. (1990) - Multivariable phase diagrams: an algorithm based on generalized thermodynamics. *American Journal of Science*, 290, 666-718.

Conrad W.K., Nicholls I.A. and Wall V.J. (1988) - Water saturated and undersaturated melting at 10 kbar: evidence for the origin of silicic magmas in the Taupo volcanic zone, New Zealand, and other occurrences. *Journal of Petrology*, 29, 765-803.

Costamagna L.G., Cruciani G., Franceschelli M. and Puxeddu M. (2012) - A volcano-sedimentary sequence with albitite layers in the Variscan basement of NE Sardinia: a petrographical and geochemical study. *Periodico di Mineralogia*, 81, 2, 179-204.

Cruciani G., Franceschelli M., Caredda A.M. and Carcangiu G. (2001) - Anatexis in the Hercynian basement of NE Sardinia, Italy: a case study of the migmatite of Porto Ottiolu. *Mineralogy and Petrology*, 71, 195-223.

Cruciani G., Franceschelli M., Elter F.M., Puxeddu M. and Utzeri D. (2008a) - Petrogenesis of Al-silicate-bearing throndhjemitic migmatites from NE Sardinia, Italy. *Lithos*, 102, 554-574.

Cruciani G., Franceschelli M. and Groppo C. (2011) - P-T evolution of eclogite-facies metabasite from NE Sardinia, Italy: insights into the prograde evolution of Variscan eclogites. *Lithos*, 121, 135-150.

Cruciani G., Franceschelli M., Groppo C. and Spano M.E. (2012) - Metamorphic evolution of non-equilibrated granulitized eclogite from Punta de li Tulchi (Variscan Sardinia) determined through texturally controlled thermodynamic modelling. *Journal of Metamorphic Geology*, 30, 667-685.

Cruciani G., Franceschelli M., Jung S., Puxeddu M. and Utzeri D. (2008b) - Amphibole-bearing migmatites from the Variscan Belt of NE Sardinia, Italy: Partial melting of mid-Ordovician igneous sources. *Lithos*, 105, 208-224.

Cruciani G., Franceschelli M., Massonne H.-J., Carosi R. and Montomoli C. (2013) - Pressure-temperature and deformational evolution of high-pressure metapelites from Variscan NE Sardinia, Italy. *Lithos*, 175-176, 272-284.

Elter F.M., Franceschelli M., Ghezzo C., Memmi I. and Ricci C.A. (1986) - The geology of northern Sardinia. In: Guide-book to the excursion on the Paleozoic basement of Sardinia. (eds.): Carmignani L., Cocozza T., Ghezzo C., Pertusati P.C. and Ricci C.A., IGCP Project No. 5, Newsletter, special issue, 87-102.

Elter F.M., Musumeci G. and Pertusati P.C. (1990) - Late Hercynian shear zones in Sardinia. *Tectonophysics*, 176, 387-404.

Elter F.M., Padovano M. and Kraus R.K. (2010) - The emplacement of Variscan HT metamorphic rocks linked to the interaction between Gondwana and Laurussia: structural constraints in NE Sardinia (Italy). *Terra Nova*, 22, 369-377.

Fettes D. and Desmons J. (2007) - Metamorphic Rocks - A Classification and Glossary of Terms. Cambridge University Press, 244 pp.

Franceschelli M., Carcangiu G., Caredda A.M., Cruciani G., Memmi I. and Zucca M. (2002) - Transformation of cumulate mafic rocks to granulite and re-equilibration in amphibolite and greenschist facies in NE Sardinia, Italy. *Lithos*, 63, 1-18.

Franceschelli M., Eltrudis A., Memmi I., Palmeri R. and Carcangiu G. (1998) - Multi-stage metamorphic re-equilibration in eclogitic rocks from the Hercynian basement of NE Sardinia (Italy).

Mineralogy and Petrology, 62, 167-193.

Franceschelli M., Memmi I., Pannuti F. and Ricci C.A. (1989) - Diachronous metamorphic equilibria in the Hercynian basement of northern Sardinia, Italy. In: Evolution of metamorphic belts. (eds): Daly J.S., Cliff R.A. and Yardley B.W.D., *Geological Society of London, Special Publications*, 43, 371-375.

Franceschelli M., Puxeddu M. and Cruciani G. (2005) - Variscan metamorphism in Sardinia, Italy: review and discussion. In: The southern Variscan belt. (eds): Carosi R., Dias R., Iacopini D. and Rosenbaum G., *Journal of the Virtual Explorer*, 19, Paper 2.

Garcìa-Casco A., Torres-Roldan R.L., Millan G., Monie P. and Haissen F. (2001) - High-grade metamorphism and hydrous melting of metapelites in the Pinos terrane (W Cuba): evidence for crustal thickening and extension in the northern Carribean collisional belt. *Journal of Metamorphic Geology*, 19, 699-715.

Ghezzo C., Memmi I. and Ricci C.A. (1979) - Un evento granulitico nel basamento metamorfico della Sardegna nord-orientale. *Memorie della Società Geologica Italiana*, 20, 23-38.

Giacomini F., Bomparola R.M. and Ghezzo C. (2005) - Petrology and geochronology of metabasites with eclogite facies relics from NE Sardinia: constraints for the Palaeozoic evolution of Southern Europe. *Lithos*, 82, 221-248.

Giacomini F., Bomparola R.M., Ghezzo C. and Guldbransen H. (2006) - The geodynamic evolution of Southern European Variscides: constraint from the U/Pb geochronology and geochemistry of the lower Paleozoic magmatic-sedimentary sequences of Sardinia (Italy). *Contributions to Mineralogy and Petrology*, 152, 19-42.

Groppo C., Rolfo F. and Lombardo B. (2009) - P-T evolution across the Main Central Thrust Zone (Eastern Nepal): hidden discontinuities revealed by petrology. *Journal of Petrology*, 50, 1149-1180.

Groppo C., Rubatto D., Rolfo F. and Lombardo B. (2010) - Early Oligocene partial melting in the Main Central Thrust Zone (Arun valley, eastern Nepal Himalaya). *Lithos*, 118, 287-301.

Helbing H. and Tiepolo M. (2005) - Age determination of Ordovician magmatism in NE Sardinia and its bearing on Variscan basement evolution. *Journal of the Geological Society of London*, 162, 689-700.

Holland T., Baker J. and Powell R. (1998) - Mixing properties and activity-composition relationships of chlorites in the system $MgO–FeO–Al_2O_3–SiO_2–H_2O$. *European Journal of Mineralogy*, 10, 395-406.

Holland T.J.B. and Powell R. (1998) - An internally consistent thermodynamic data set for phases of petrological interest. *Journal of Metamorphic Geology*, 16, 309-343.

Holland T. and Powell R. (2001) - Calculation of phase relations involving haplogranitic melts using an internally consistent thermodynamic dataset. *Journal of Petrology*, 42, 673-683.

Johnson T. and Brown M. (2004) - Quantitative constraints on metamorphism in the Variscides of Southern Brittany - a complementary pseudosection approach. *Journal of Petrology*, 45, 1237-1259.

Johnson T.E., Gibson R.L., Brown M., Buick I.S. and Cartwright I. (2003) - Partial melting of metapelitic rocks beneath the Bushveld Complex, South Africa. *Journal of Petrology*, 44, 789-813.

Jung C., Jung S., Nebel O., Hellebrand E., Masberg P. and Hoffer E. (2009) - Fluid-present melting of meta-igneous rocks and the generation of leucogranites - Constraints from garnet major- and trace element data, Lu-Hf whole rock-garnet ages and whole rock Nd-Sr-Hf-O isotope data. *Lithos*, 111, 220-235.

Jung S., Mezger K., Masberg P., Hoffer E. and Hoernes S. (1998) - Petrology of an intrusion-related high-grade migmatite: implications for partial melting of metasedimentary rocks and leucosome-forming processes. *Journal of Metamorphic Geology*, 16, 425-445.

Korhonen F.J., Saito S., Brown M. and Siddoway C.S. (2010) - Modeling multiple melt loss events in the evolution of an active continental margin. *Lithos*, 116, 230-248.

Massonne H.-J., Cruciani G. and Franceschelli M. (2013) - Geothermobarometry on anatectic melts - a high-pressure Variscan migmatite from northeast Sardinia. *International Geology Review*, 55, 1490-1505.

Newton R.C., Charlu T.V. and Kleppa O.J. (1981) - Thermochemistry of the high structural state plagioclases. *Geochimica et Cosmochimica Acta*, 44, 933-941.

Padovano M., Elter F.M., Pandeli E. and Franceschelli M. (2012) - The East Variscan shear zone: new insights into its role in the Late Carboniferous collision in southern Europe. *International Geology Review*, 54, 957-970.

Palmeri R. (1997) - P-T paths and migmatite formation: an example from Deep Freeze Range, northern Victoria Land, Antarctica. *Lithos*, 42, 47-66.

Powell R. and Holland T. (1999) - Relating formulations of the thermodynamics of mineral solid solutions: Activity modeling of pyroxenes, amphiboles, and micas. *American Mineralogist*, 84, 1-14.

Ricci C.A., Carosi R., Di Vincenzo G., Franceschelli M. and Palmeri R. (2004) - Unravelling the tectono-metamorphic evolution of medium-pressure rocks from collision to exhumation of the Variscan basement of NE Sardinia (Italy): a review. *Periodico di Mineralogia*, 73, 73-83.

Sawyer E.W. and Barnes S.J. (1988) - Temporal and compositional differences between subsolidus and anatectic migmatite: leucosomes from the Quetico metasedimentary belt, Canada. *Journal of Metamorphic Geology*, 6, 437-450.

Taylor J. and Stevens G. (2010) - Selective entrainment of peritectic garnet into S-type granitic magmas: evidence from Archaean mid-crustal anatectites. *Lithos*, 120, 277-292.

Thompson J.B. and Hovis G.L. (1979) - Entropy of mixing in sanidine. *American Mineralogist*, 64, 57-65.

White R.W., Powell R. and Holland T.J.B. (2001) - Calculation of partial melting equilibria in the system Na_2O-CaO-K_2O-FeO-MgO-Al_2O_3-SiO_2-H_2O (NCK FMASH). *Journal of Metamorphic Geology*, 19, 139-153.

Wimmenauer W. (1984) - Das praevariszische Kristallin im Schwarzwald. *Fortschritte der Mineralogie: Beiheft,* 62, 69-86.

Submitted, October 2013 - Accepted, January 2014